p27Kip1 in cell-cell adhesion and cell polarity

Theard, Delphine Francine

Chapter 2

Oncostatin M-Stimulated Apical Plasma Membrane Biogenesis Requires $p27^{Kip1}$-Regulated Cell Cycle Dynamics

Sven C. D. van IJzendoorn[1], Delphine Théard[1], Johanna M. van der Wouden, Willy Visser, Kacper A. Wojtal and Dick Hoekstra
[1] *These authors contributed equally.*

Department of Membrane Cell Biology, University of Groningen, Antonius Deusinglaan, 1, 9713 AV, Groningen, The Netherlands

Published in Mol Biol Cell. 2004 Sep;15(9):4105-14.

Abstract

Oncostatin M regulates membrane traffic and stimulates apicalization of the cell surface in hepatoma cells in a protein kinase A-dependent manner (van der Wouden et al., 2002). Here, we show that oncostatin M enhances the expression of the cyclin-dependent kinase (cdk)2 inhibitor p27^{Kip1}, which inhibits G_1-S phase progression. Forced G_1-S-phase transition effectively renders pre-synchronized cells insensitive to the apicalization-stimulating effect of oncostatin M. G_1-S-phase transition prevents oncostatin M-mediated recruitment of protein kinase A to the centrosomal region, and precludes the oncostatin M-mediated activation of a protein kinase A-dependent transport route to the apical surface, which exits the subapical compartment (SAC). This transport route has previously been shown to be crucial for apical plasma membrane biogenesis. Taken together, our data indicate that oncostatin M-stimulated apicalization of the cell surface is critically dependent on the ability of oncostatin M to control p27^{Kip1}/cdk2-mediated G_1-S-phase progression, and suggest that the regulation of apical plasma membrane-directed traffic from SAC and centrosome dynamics are coupled.

Introduction

The establishment and maintenance of apical and basolateral plasma membrane (PM) domains in epithelia requires a careful orchestration of extra- and intracellular signals, triggering crucial cytoskeleton, organelle- and membrane traffic-linked machineries, as partly elucidated in systems as diverse as yeast, Drosophila and mammalian cells (Mostov et al., 2003; Lecuit and Pilot, 2003; Baas et al., 2004). Impairment of these events may cause a loss of apical-basolateral asymmetry and may lead to deranged cell growth (Bilder et al., 2000; Vermeer et al., 2003; Baas et al., 2004) or spindle misorientation (Albertson and Doe, 2003). Recent studies have reported an evolutionary conserved genetic program that may link the process of polarity deveopment and proliferation (Bilder et al., 2000; Rolls et al. 2003; Humbert et al., 2003; Klezovitch et al., 2004). However, many aspects of such a link remain unclear, e.g. the extent to which cell proliferation can directly affect epithelial cell organization or vice versa. Indeed, epithelial cell proliferation and apical-basolateral polarity may be controled by different signaling pathways (Liu et al., 2004).

Signaling cascades stimulated by IL-6 family cytokines, including oncostatin M (OSM), elicit multiple responses in the cell. Originally, as its name indicates, oncostatin M was primarily recognized to inhibit the proliferation of tumor cells (Tanaka and Miyajima, 2003), presumably by modulating cell cycle regulatory proteins including the cyclin-dependent kinase (cdk)2-inhibitor $p27^{Kip1}$ (Kortylewski et al., 1999; Klausen et al., 2000; Li et al., 2001). Disruption of the regulatory system that controls G_1 phase progression is a common event in human hepatocarcinogenesis (Hui et al., 1998), and $p27^{Kip1}$ has been associated with differentiation, invasiveness and metastasis of hepatocellular carcinoma tumors (Zhou et al., 2003). Recent evidence indicate that OSM signaling plays a prominent role in liver development (Kamiya et al., 1999; 2001; 2002; Kojima et al., 2000; Kinoshita

and Miyajima, 2002; Matsui et al., 2002; Hanada et al., 2003; Lazaro et al., 2003; Chagraoui et al., 2003). OSM stimulates hepatocyte nuclear factor-4 (Kamiya et al., 2003), which may integrate the genetic programs of liver-specific gene expression and epithelial morphogenesis (Spath and Weiss, 1998). In addition, OSM induces adherens junction formation by altering the subcellular localization of adherens junction components including E-cadherin and catenins (Matsui et al., 2002). In human fetal hepatocytes as well as in well-differentiated human hepatic HepG2 cells, OSM stimulates the development of apical, bile canalicular plasma membrane (PM) domains (Lazaro et al., 2003; van der Wouden et al, 2003), which requires the activation of a gp130-mediated signaling cascade and endogenous protein kinase A (PKA) activity (van der Wouden et al., 2002). Although the molecular mechanisms that underlie apicalization of the cell surface in hepatocytes are poorly understood, the *de novo* reorganization of the lateral PM following the establishment of E-cadherin-dependent cell-cell adhesion, mediated by cytoskeleton rearrangements and the polarized sorting and trafficking of proteins and lipids, plays a crucial role.

Apical protein and lipid sorting in polarized hepatocytes occurs in the Golgi apparatus and the subapical compartment (SAC; the hepatocyte equivalent of the pericentriolar recycling endosomes in other epithelia). In the Golgi apparatus, newly synthesized proteins and lipids destined for the apical surface are sorted into sphingolipid-cholesterol-enriched membrane microdomains (rafts). Thus, in the trans-Golgi network, multi membrane-spanning or polytopic apical membrane proteins are clustered in Lubrol WX-resistant membrane domains and delivered via vesicular transport directly to the apical surface (Slimane et al., 2003). Single membrane-spanning apical proteins are segregated in other, Triton X-100-resistant membrane domains and targeted first to the basolateral surface, followed by their transport to the apical domain by transcytosis (Slimane et al., 2003; Nyasae et al., 2003; Tuma and Hubbard, 2003). Following

surface delivery extensive membrane exchange occurs between the apical and basolateral domains, which involves endocytosis and subsequent recycling to either PM domain. The SAC plays a prominent role in the polarized delivery of proteins and lipids and, thus, in maintaining cell surface polarity (Ihrke et al. 1998; van IJzendoorn and Hoekstra, 1999; van IJzendoorn et al., 1999; Rahner et al., 2000; van IJzendoorn and Mostov, 2000). Moreover, polarized membrane traffic from SAC is also important for the *de novo* biogenesis of apical PM domains (van IJzendoorn and Hoekstra, 2000), triggered by extracellular stimuli, including OSM (van der Wouden et al., 2002) and those that elicit cAMP/protein kinase A (PKA) signaling cascades (Zegers and Hoekstra, 1998). Indeed, we have previously shown that OSM activates a vesicular membrane trafficking pathway from SAC to the apical PM, and dependent on cAMP/ PKA activity (van der Wouden et al., 2002). Importantly, activation of this OSM-cAMP/PKA-regulated pathway is crucial for apical PM biogenesis in HepG2 cells (van der Wouden et al., 2002).

The pronounced effects of OSM on cell cycle progression, membrane traffic and cell polarity prompted us to investigate the functional relationship between these events in order to obtain better insight into molecular mechanisms that control the establishment of apical surface domains in conjunction with cell cycle control.

Materials and Methods

Cell culture

HepG2 cells were grown in DMEM with 4500 mg of glucose per liter, containing 10% fetal calf serum and antibiotics. Media were changed every other day. Cells were trypsinized after reaching confluency. For experiments, cells were plated at low density onto ethanol-sterilized coverslips and analyzed 24, 48, 72, or 76 h after plating.

In order to synchronize cells in the G_1 phase of the cell cycle, cells were first grown in normal culture medium for 36 h to allow expansion of the cells, followed by culture in serum-free medium for 36 h. In some experiments, cells were subsequently exposed to normal culture medium containing 10% FCS, or cultured in medium supplemented with 30 µM fumonisin B1 (Sigma, St.Louis/OR; see Results), to chase the cells from G_1 into the S-phase. As a control, cells were chased in serum-free medium. G_1-S-phase transition was monitored by the initiation of DNA synthesis, as evidenced by BrdU incorporation (Figures 2C and 3C). In other experiments, cells were first grown in normal culture medium for 36 h, followed by culturing in normal medium supplemented with the DNA synthesis inhibitor hydroxyurea (4 mM; Sigma, St.Louis/OR) to synchronize the cells in S-phase.

Determination of HepG2 cell polarity

Accurate estimation of the degree of HepG2 polarity was performed as described elsewhere (Zegers and Hoekstra, 1997; van IJzendoorn and Hoekstra, 2000). Briefly, the cells were fixed with –20°C ethanol for 10 s, rehydrated in HBSS, and subsequently incubated with a mixture of TRITC-labeled phalloidin (Molcular Probes, Eugene/OR) and 5 ng/ml of the nuclear stain Hoechst 33528 (Sigma, St.Louis/MO) at room temperature for 30 min. The cells were then washed and the number of bile canaliculi (BC; identified by the presence of dense F-actin staining around the BC) per 100 cells (identified by fluorescently labeled nuclei) was determined and expressed as the ratio [BC/100 cells]. Ten fields (each containing >50 cells) per coverslip (at least two coverslips per condition were studied) were

analyzed. Cells were examined using an epifluorescence microscope (Provis AX70, Olympus corp., New Hyde Park, NY).

Immunostaining of HepG2 cells

HepG2 cells were fixed in 4% PFA for 30 min at room temperature, washed and permeabilized for 10 min with methanol at –20°C. After blocking with 1% BSA in phosphate-buffered saline (37°C; 1 h) the cells were incubated with primary antibody for 1 h at 37°C. For immunofluorescent co-staining of γ-tubulin and PKA, cells were first incubated with 0.5% Triton X100 at 4°C for 3 min, followed by fixation with ice-cold (-20°C) methanol for 5 min and blocking with 1% BSA. Monoclonal anti-p27Kip1 and anti-PKA-RIIα antibodies were bought from Transduction Laboratories and used at 1:300 dilution. Following incubation with the primary antibodies, cells were washed and incubated with the corresponding secondary antibody labeled with Alexa Fluor^{488} or Alexa Fluor^{594} (Molecular Probes, Eugene/OR) for 30 min at room temperature. The coverslips were mounted and analyzed by confocal microscopy (Leica TCS SP2; Germany).

BrdU incorporation assay

HepG2 cells were incubated with 50 mM bromodeoxyuridine (BrdU) in normal culture medium (see Results). Cells were then washed with HBBS and fixed with 4% paraformaldehyde (PFA) at room temperature for 30 min. Cells were subsequently washed with HBBS and incubated in 2 N HCl for 1 h. Cells were processed for immunofluorescence microscopy as described above. In brief, cells were incubated at 37°C for 30 min with a mouse mAb against BrdU (Chemicon, 1:50 dilution). As secondary antibody, Alexa^{488} goat anti-mouse IgG was used (Molecular Probes, Eugene/OR). During the secondary antibody incubation, 5 ng/ml of the nuclear stain Hoechst 33528 was included to visualize the nuclei. The cells were then rinsed 4 times with HBBS, mounted, and examined by fluorescence microscopy as described above. The percentage of cells that had incorporated BrdU was quantified by determining the ratio of BrdU-positive nuclei. At least 10 fields each containing > 50 cells were counted.

Analysis of p27^{Kip1} Levels by Western Blot

HepG2 cells were treated as described in the Results section, and then lysed in 0.5 ml of Triton X-100 lysis buffer (10 mM triethanolamine, pH 7.4, 1.0% Triton X-100, 0.1% SDS, 100 mM NaCl, 1 mM EDTA, 1 mM EGTA, 1 mM NaF, 20 mM Na_4P2O_7 and 2 mM sodium vanadate and a cocktail of protease inhibitors). Lysates were boiled for 5 min and cleared by centrifugation. Protein concentrations were determined by a bicinchoninic acid (BCA) protein assay (Sigma), and equal amounts of proteins were separated on 10% SDS-PAGE gels, immunoblotted with monoclonal p27^{Kip1} antibodies (Transduction Laboratories), and detected with an enhanced chemiluminescence system (Amersham Biosciences). Bands representing p27^{Kip1} were quantified using Scion Image software.

Analysis of transport of C_6-NBD-GalCer from SAC

In order to study the trafficking of the fluorescent GalCer analog from SAC, SAC were preloaded with the lipid as depicted in Figure 1. This procedure has been described in detail previously (van IJzendoorn and Hoekstra, 1999; 2000). In short, cells were labeled with 4 µM C_6-NBD-GalCer at 37°C (Figure 1, step 1) to allow internalization from the basolateral surface and subsequent transcytosis to the apical, bile canalicular PM domain (BC; Figure 1, step 2). After 30 min of incubation, lipid analog still residing at the basolateral domain was depleted by a back exchange procedure at 4°C (2 x 30 min incubation in HBSS + 5% w/v bovine serum albumin (BSA; Fluka Chemie, Fuchs/Switzerland); c.f. van IJzendoorn et al., 1997) (Figure 1, step 3), and BC-associated lipid analog was chased into SAC at 18°C for 1 h in back exchange medium (Figure 1, step 4). Then, the NBD-fluorescence at the exoplasmic BC leaflet was abolished using sodium dithionite (Merck, Darmstadt/Germany) at 4°C, leaving the vast majority of the intracellular GalCer analog in SAC (Figure 1, step 5; van IJzendoorn and Hoekstra, 1998; 2000). After removal of dithionite by washing, transport from SAC was examined by incubating in back exchange medium at 37°C (Figure 1, step 6).

In order to quantitate transport of the lipid analog to and from the BC, the percentage of NBD-positive BC was determined as described elsewhere (van IJzendoorn et al., 1997; van IJzendoorn and Hoekstra, 1998). Briefly, BC were first identified

by phase contrast illumination, and then categorized as NBD-positive or NBD-negative under epifluorescence illumination. Note that a BC is categorized as fluorescently labeled, i.e. NBD-positive, when microvilli-like structures, characteristic of the BC, can be detected that are seemingly fluorescent in the wake of the fluorescence derived from the lipid analog, present in the apical membrane (van IJzendoorn et al., 1997). Such microvilli-like structures are typically and readily observed upon gradual photobleaching of the BC-associated NBD fluorescence.
Distinct pools of fluorescence are thus discerned at the apical pole of the cells, present in vesicular structures adjacent to BC, which are defined as subapical compartments (SAC, c.f. van IJzendoorn and Hoekstra, 1998). Together, BC and SAC constitute the BCP in HepG2 cells (see Figure 1). Therefore, within the BCP region the localization of the fluorescent lipid analog will be defined as being derived from the BC, SAC or both. This also provides a means to describe the movement of the lipid within or out of this region in the cell (van IJzendoorn and Hoekstra, 1999). Thus, after loading SAC with lipid analog and allowing its transport to take place as described above, the direction of movement of the lipid from or within the BCP region is determined after a given time, by establishing the distribution of the NBD-labeled lipid over the various compartments (BC, SAC or both) that constitute the BCP, relative to the labeling (i.e. primarily SAC), prior to starting the chase ($t = 0$). For this kind of analysis, at least 50 BCP per coverslip were analyzed. Data are expressed as the mean ± SEM of at least four independent experiments, carried out in duplicate and Student's *t*-tests were carried out to determine the statistical significance of the data.

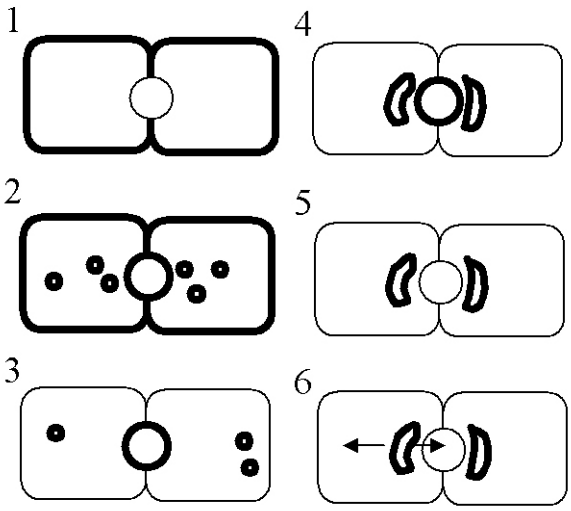

Figure 1 Schematic representation of the various steps of the lipid transport assays. The cell-labeling situation after the corresponding incubation step is depicted at the right. Cells are incubated with C_6NBD-GalCer at 37°C for 30 min, which allows incorporation of the probe in the basolateral plasma membrane (step 1) and subsequent transcytosis to the apical domain (BC; step 2). Then, the fraction of the fluorescent lipid probe still residing at the basolateral PM is depleted by BSA at 4°C twice for 30 min (step 3). The BC-associated probe is then chased into SAC at 18°C for 1 h in BSA-containing medium (step 4). The presence of BSA in the medium during this step will prevent reentry of any C_6NBD-GalCer that might arrive basolaterally during the chase. Next, the probe remaining at the BC is quenched by sodium dithonite (step 5). The sodium dithionite is removed by extensive washing with ice-cold HBSS. Occasionally, cells were subsequently incubated with OSM at 4°C for 30 min. Transport of the subapically derived fluorescent probe can be monitored upon rewarming and incubating the cells at 37°C (step 6).

Results

Cell polarity development is positively correlated with $p27^{Kip1}$ expression

Well-differentiated human hepatic HepG2 cells have been successfully employed for the study of membrane dynamics and polarity development in hepatocytes. Apical, bile canalicular PM domains (BC) form between two adjacent cells, as readily visualized by staining the underlying actin network with fluorescently-labeled phalloidin (van IJzendoorn et al., 1997). As shown in figure 2A, HepG2 cells acquire plasma membrane (PM) polarity in time, as evidenced by the ratio BC/100 cells, and reach optimal polarity 3 days after plating (Figure 2A; c.f. van IJzendoorn and Hoekstra, 2000). Treatment of the cells with dibutyryl (db) cAMP or the interleukin-6 family cytokine oncostatin M stimulates polarity development, i.e. apical PM biogenesis in HepG2 cells (Figure 2A, black bars and grey bars, respectively, c.f. van der Wouden et al., 2002), as evidenced by a 2.4- and 1.5-fold increase in the ratio BC/100 cells at 24 and 48-72 h, respectively, following plating. Similar results were obtained with other stable cAMP analogs, and the adenylate cyclase agonist forskolin, but not with sodium butyrate (data not shown; c.f. Zegers and Hoekstra, 1997).

Although the process of cell differentiation generally appears negatively correlated with cellular proliferation, it is not clear whether cell polarity and proliferation are directly, e.g. genetically, linked or that one is an indirect by-effect of the other. We observed that following plating, the expression of $p27^{Kip1}$ increases significantly (approximately 2-fold) during the first 48 h, after which it remains at a constant level (Figure 2B; 2C, white bars). $p27^{Kip1}$ plays a critical role in mediating cell cycle exit by inhibiting the activity of cyclinE/cdk2, a kinase that is required for the transition of cells from the G_1 phase, i.e. the gap between mitosis and the next round of DNA synthesis, into S-phase. In agreement with the observed increase in $p27^{Kip1}$ expression, the

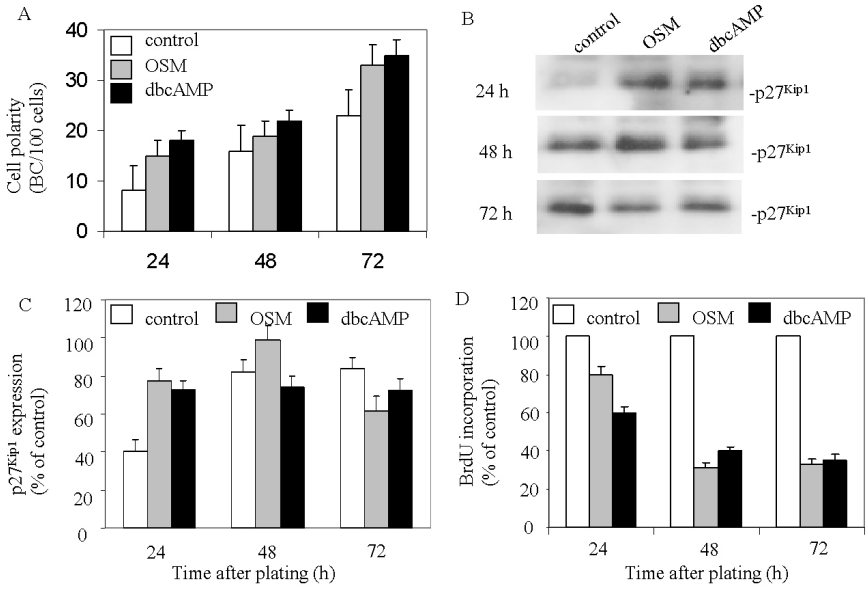

Figure 2 Cell polarity development is positively correlated to p27^{Kip1} expression and G_1 phase arrest. A. The ratio BC/100 cells was determined at different times in cells cultured on coverslips in normal culture medium (white bars), or normal culture medium supplemented with OSM (grey bars) or dibutyryl (db)cAMP (black bars). B. Cells were cultured in medium supplemented or not with OSM or dbcAMP for different times. Cells were then lysed and p27^{Kip1} expression was examined by western blot. A representative blot of three independent experiments is shown. C. Expression levels of p27Kip1 (as depicted in B) were quantified using Scion Image software. The percentage increase compared to non-treated cells (set to 100%) of three independent experiments is shown. D. Cells were cultured in black bars) for different times. 24 h prior to analysis, BrdU was included in the culture medium. Cells were fixed and stained with anti-BrdU antibodies and the DNA stain Hoechst for immunofluorescence analysis. Note the decreased incorporation of BrdU in OSM- and dbcAMP-treated cells when compared to control cells (set to 100%), indicative for inhibited G_1-S-phase transition.

number of cells that enter S-phase and start DNA synthesis is reduced, as evidenced by a decreased incorporation of the thymidine analog bromodeoxyuridine (BrdU). Treatment of the cells with oncostatin M (10 ng/ml) enhances the increase in $p27^{Kip1}$ expression during the first 48 h (Figure 2B; 2C, grey bars) and results in a more pronounced arrest in the G_1 phase (Figure 2D, grey bars). Similar results were obtained with dibutyryl cAMP (Figure 2B, C and D, black bars), well-known to stimulate cell polarity development (Figure 2A, black bars; c.f. Zegers et al., 1997; van IJzendoorn and Hoekstra, 1999; 2000), and following serum deprivation (see Figure 3). Taken together, oncostatin M- and cAMP-stimulated cell polarity, i.e. apical PM biogenesis, is positively correlated with $p27^{Kip1}$ expression and G_1-phase arrest.

Downregulation of $p27^{Kip1}$ expression and subsequent S-phase entry inhibits oncostatin M- stimulated polarity development

We next investigated whether control of G_1-S phase progression by $p27^{Kip1}$ is functionally coupled to apical PM biogenesis. To this end, cells were cultured for 36 h in normal cell culture medium to allow expansion of the cells, followed by serum-deprivation for another 36 h to synchronize the cells in the G_1 phase. Cells were then stimulated with medium supplemented with or without (control) 10% FCS and oncostatin M, in the presence of BrdU for 4 h (Figure 3A). As shown in Figure 3B and C, serum deprivation resulted in increased levels of $p27^{Kip1}$ (~1.4-fold), whereas the subsequent stimulation with serum, but not buffer, resulted in the marked downregulation of $p27^{Kip1}$ expression (~40%). In agreement with this, few cells entered S-phase in serum-deprived cells whereas, by contrast, >70% of the cells (~3.5 fold increase) entered S-phase following serum stimulation, as evidenced by a massive BrdU incorporation (Figure 3D). The mitotic index in serum-stimulated cell cultures was <3% (data not shown). Importantly, whereas oncostatin M effectively stimulated cell polarity development in serum-

deprived cells by ~45%, as evidenced by an increased ratio of apical PM domains per number of cells, serum-stimulated cells were found to be completely insensitive to oncostatin M stimulation with respect to apical PM biogenesis (Figure 3E).

As an alternative approach to drive cells from G_1 into the S-phase, the cells were treated with the mycotoxin fumonisin B1 (FB1) which, in HepG2 cells, results in a decrease in $p27^{Kip1}$ expression of approximately 75% (Figure 4A, manuscript in preparation). As a consequence, cells treated with FB1 shifted from the G_1 to S-phase, evidenced by an increase in the number of cells that had incorporated BrdU (Figure 4A, insert). Treatment of the cells with FB1 inhibits polarity development which can be contributed to elevated levels of sphinganine (Figure 4B; van IJzendoorn et al., manuscript submitted). We then examined the effect of FB1-mediated downregulation of $p27^{Kip1}$ expression on the ability of oncostatin M to stimulate apical PM biogenesis. Oncostatin M failed to stimulate polarity development in FB1-treated cells (Figure 4B), similarly as observed in serum-stimulated cells (Figure 3D).

Downregulation of $p27^{Kip1}$ expression and subsequent G_1-S-phase transition is typically mediated by the increased activity of cyclin-dependent kinase2 (cdk2). Indeed, when serum-deprived cells were incubated with the cdk2 inhibitor roscovitin during subsequent serum-or FB1-stimulation, cells failed to enter S-phase, as evidenced by a lack of increased BrdU incorporation (not shown). Importantly, cdk2-inhibited cells retained their sensitivity to the polarity-stimulating effects of oncostatin M following serum- or FB1-stimulation (Figure 3E, 4B). These data thus suggest that $p27^{Kip1}$ downregulation by itself is not sufficient, but requires cdk2 activity to render the cells insensitive to the polarity-stimulating effects of oncostatin M. Conversely, the downregulation of cdk2 activity, mediated by OSM-stimulated $p27^{Kip1}$ expression, thus appears an important parameter in OSM-stimulated apical PM biogenesis.

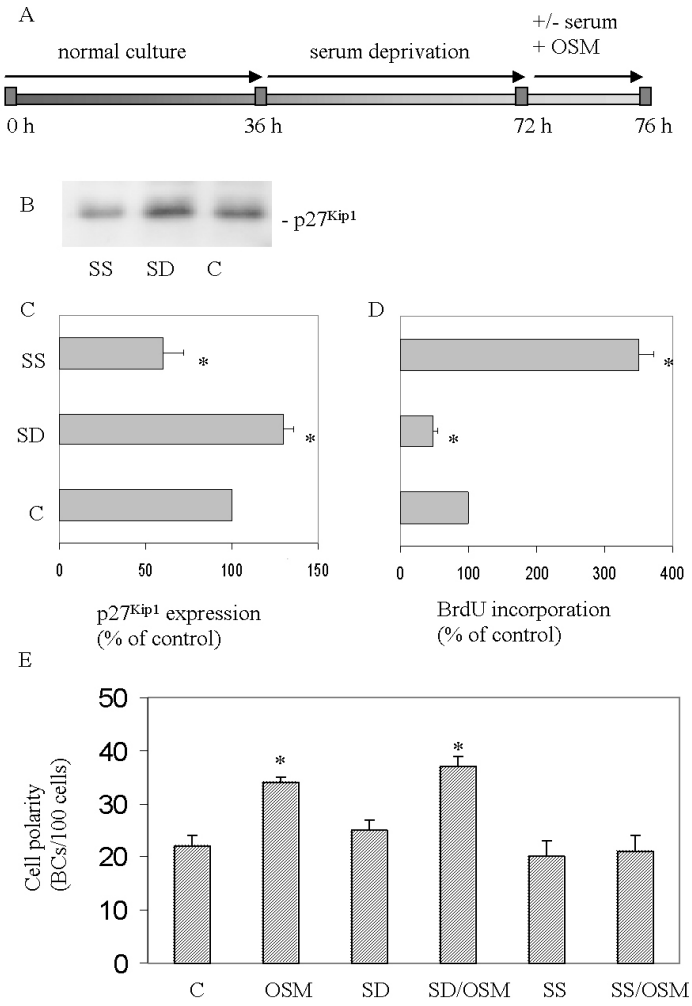

Figure 3 Effect of OSM on polarity development in G_1 and S-phase HepG2 cells. A. Scheme depicting how cells are synchronized and treated with OSM in the G_1 and S-phase of the cell cycle. B. Expression levels of $p27^{Kip1}$ in serum-deprived (SD), serum-stimulated (SS) and control (C) cells. C. Quantification of the relative expression levels of $p27^{Kip1}$ in serum-deprived (SD), serum-stimulated (SS) compared to control (C) cells. D. Relative changes in the incorporation of BrdU in serum-deprived (SD), serum-stimulated (SS) compared to control (C) cells. E. Effect of OSM on polarity development in serum-deprived (SD), serum-stimulated (SS) and control (C) cells

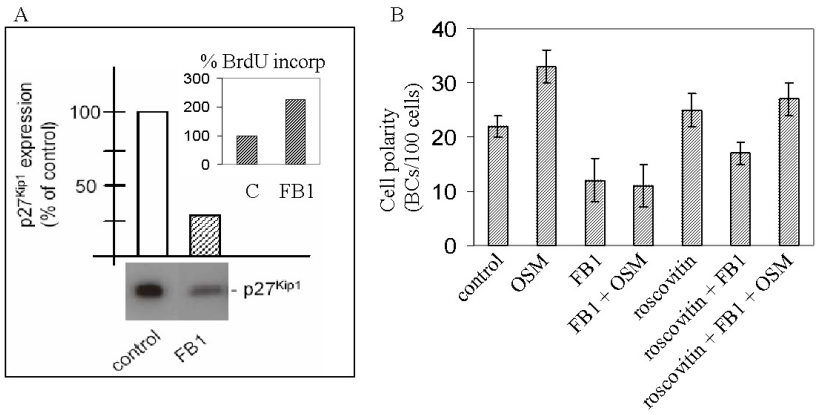

Figure 4 Effect of Fumonisin B1 (FB1) on cell cycle and OSM-mediated polarity development. A. FB1 downregulates $p27^{Kip1}$ expression (blot and quantification) and promotes S-phase entry, as evidenced by BrdU incorporation (insert). B. FB1 inhibits OSM-stimulated polarity development in HepG2 cells. Note that the cdk2 inhibitor roscovitin restores the stimulatory effect of OSM on polarity development in FB1-treated cells.

Initiation of DNA synthesis is not responsible for the attenuation of oncostatin M stimulation of cell polarity development

Transition of cells from G_1 to S-phase is accompanied by two key events: initiation of DNA synthesis and centriole duplication, both of which are under strict control of cdk2 and $p27^{Kip1}$, but can occur independently of each other. In order to determine whether the ability of cells to respond to OSM in terms of polarity development is specifically related to either of these two events, we employed hydroxyurea ($CH_4N_2O_2$). Hydroxyurea inactivates ribonucleoside reductase, thereby blocking deoxynucleotide synthesis which inhibits DNA synthesis, but does not block centrosome duplication (Balczon et al., 1995; Khodjakov et al., 2002). HepG2 cells were cultured for 36 h in normal culture medium to allow expansion of the cells, and then treated with 4 mM hydroxyurea for 36 h, followed by incubation in medium

containing OSM and hydroxyurea for 4 h (Figure 5A). Hydroxyurea prevented DNA synthesis in HepG2 cells as evidenced by reduced BrdU incorporation compared to non-treated cells (73% reduction; c.f. Chouteau et al., 2001). As shown in Figure 5B, hydroxyurea rendered the cells insensitive to the polarity-stimulating effects of OSM very similar as observed in serum- or FB1-stimulated cells (c.f. Figure 3D, 4B). This suggests that the acquired insensitivity of the cells to OSM following G_1-S-phase progression can not be attributed to DNA synthesis. These data point to the intriguing possibility that cdk2-regulated centrosome cycle progression at the G1-S-phase border renders the cells insensitive to the polarity-stimulating effects of OSM.

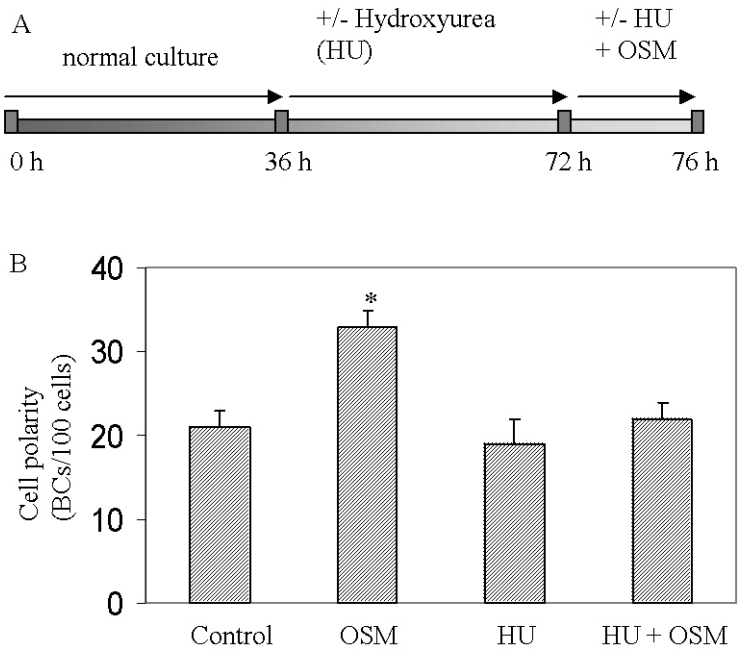

Figure 5 Effect of hydroxyurea (HU) on OSM-stimulated polarity development. A Scheme depicting how cells are synchronized with HU (4 mM). B. HU inhibits the cell polarity-stimulating effects of OSM.

G_1-S phase transition pertubs oncostatin M-regulated polarized membrane trafficking

Many organelles involved in distributing endomembranes are positioned close to the centrosome in epithelial cells. Among these are the Golgi apparatus and the pericentrosomal recycling endosome, or common endosome. The hepatocyte equivalent of the common endosome is the subapical compartment, SAC (van IJzendoorn and Hoekstra, 1999; van IJzendoorn et al., 2000). In previous studies, we have demonstrated that polarity development in HepG2 cells requires the activation of a vesicular trafficking route exiting SAC and directed towards the developing BC, which can be monitored by the flow of the fluorescent probes C_6-NBD-SM and C_6-NBD-GalCer (van IJzendoorn and Hoekstra, 1999; 2000). Oncostatin M activates this pathway to stimulate apical PM biogenesis (van der Wouden et al., 2002). The question thus arises whether upregulation of $p27^{Kip1}$ expression and, consequently, inhibition of G_1-S-phase transition, is required for oncostatin M to exert its effects on membrane traffic. To investigate this, cells were synchronized using serum-deprivation/ stimulation, according to the incubation scheme depicted in figure 3A, and SAC was preloaded with C_6-NBD-GalCer as described in detail in Materials and Methods (c.f. van der Wouden et al., 2002). A scheme depicting the incubation steps is shown in figure 1. Note that the trafficking steps necessary for loading SAC, i.e. basolateral endocytosis, apical delivery and apical PM-to-SAC transport, were not visibly affected by the synchronization procedure (Figure 6A, D). Following loading of the fluorescent lipid analogue in SAC, cells were treated with oncostatin M or medium at 4 ºC (following step 5 in figure 1), warmed to 37ºC, and lipid flow from SAC to either apical (BC) or basolateral membrane was followed for 20 min in serum-free medium or normal culture medium (Figure 1, step 6). In control (i.e. serum-deprived; G_1) cells, C_6-NBD-GalCer disappeared during this time interval from the bile canalicular pole (BCP), which comprises SAC (where the lipid is located at t=0; Figure 6A) and BC.

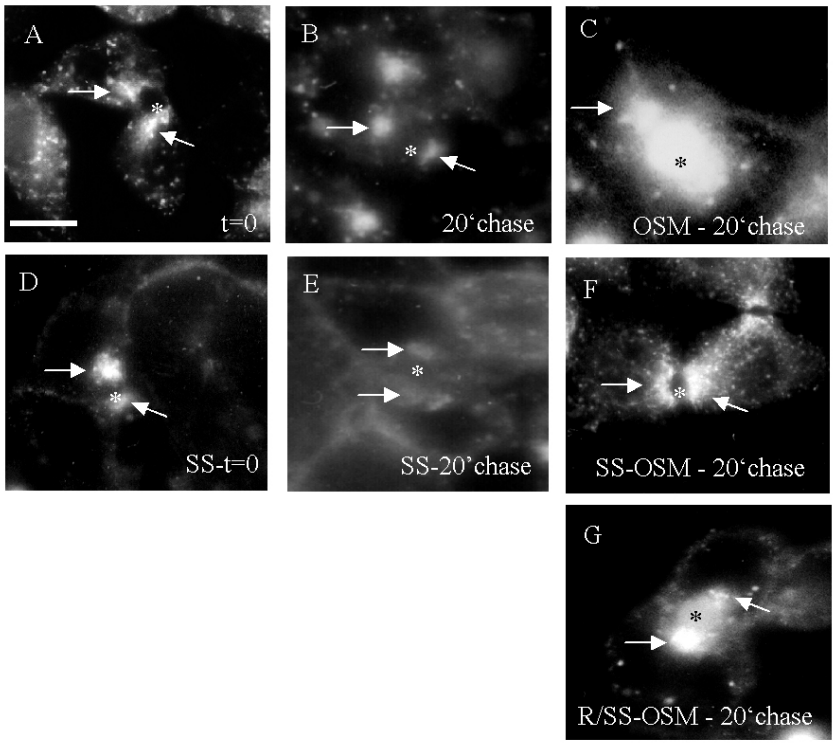

Figure 6 G_1-S-phase transition perturbs OSM-stimulated polarized membrane traffic from SAC. Serum-deprived cells kept in serum-free medium (G_1) or were stimulated with serum (SS; S-phase) after which the SAC was loaded with C_6NBD-GalCer as described in detail in Materials and Methods. Note that the fluorescent probe predominantly labeled the SAC (arrows), while no labeling of the BC (asterix) membrane was observed. In some experiments (7G), cells were then treated with roscovitin (R) for 30 min at 4°C. The fluorescent probe was subsequently chased from the SAC in serum-free (7B, C) or medium supplemented with serum (SS, 7E-G) in the presence (7C,F,G) or absence (7B,E) of OSM for 20 min at 37°C. Note the redistribution of the fluorescent probe from the SAC to the BC membranes in 7C and G, whereas no redistribution from SAC to BC could be observed in 7B, C and F. Bar 5 µm.

Indeed, the percentage of BCP that contained C_6-NBD-GalCer decreased in time (table 1). The relative distribution of the lipid analogue in the remaining, faintly-labeled C_6-NBD-GalCer - positive BCP shows that the probe predominantly resided in SAC and little if any movement from SAC to BC could be detected (table 1; Figure 6B, compare to 6A). Rather, these data indicate that the probe was transported from SAC to the basolateral domain of the cells, consistent with previous observations (van IJzendoorn and Hoekstra, 1999; 2000). By contrast, in oncostatin M-treated G_1 cells, C_6-NBD-GalCer remained associated with the BCP region during the 20 min chase, as evidenced by the unchanged percentage of BCP that contained C_6-NBD-GalCer (table 1). Analysis of the corresponding relative distribution of the probe in the BCP reveals a flow of the lipid analogue from SAC to BC (table 1; Figure 6C, compare to 6B; cf. van IJzendoorn and Hoekstra, 1999; 2000). In striking contrast, oncostatin M failed to target C_6-NBD-GalCer from SAC to BC in serum-stimulated cells, i.e. cells that had entered S-phase (table 1; Figure 6F, compare to 6E). Thus, in serum-stimulated cells, C_6-NBD-GalCer remained associated with the BCP during the 20 min chase (table 1), and analysis of the relative distribution of the lipid analogue in the labeled BCP revealed that most C_6-NBD-GalCer localized to SAC (table 1; Figure 6F), indicating entrapment of the lipid in SAC. Serum stimulation did not affect transport of the fluorescent lipid exiting SAC in the basolateral direction (Figure 6E vs. 6B). These data strongly suggest that a minimal level of $p27^{Kip1}$ expression, sufficient for G_1 arrest, is a prerequisite for oncostatin M signaling to specifically activate SAC-to-BC trafficking route and, in this way, to stimulate polarity development.

Treatment of the cells with the cdk2 inhibitor roscovitin shortly before and during serum-stimulation, thereby precluding G_1-S phase transition, rescued the ability of OSM to activate SAC-to-BC route followed by C_6-NBD-GalCer (table 1; Figure 6G, compare to 6C and 6F) and, presumably in this way, apical

PM biogenesis (Figure 4), implicating the involvement of cdk2 activity.

	0'	chase20' G_1-control	chase20' G_1-OSM	chase20' SS-OSM	chase20' R/SS-OSM
% positive BCP	89 (2)	63 (4)*	88 (3)	90 (2)	84 (4)
Rel. distr. in BCP					
SAC	84 (3)	79 (3)	40 (2)*	89 (3)	30 (4)*
BC+SAC	17 (2)	21 (3)	30 (4)*	11 (2)	20 (1)
BC	3 (1)	2 (1)	35 (3)*	3 (1)	45 (3)*

* $p < 0.05$

Table 1 G_1-S-phase transition perturbs OSM-stimulated polarized membrane traffic from SAC. Semi-quantitative analysis of the effects of cell cycle dynamics on polarized trafficking of C_6NBD-GalCer from the SAC. Serum-deprived cells kept in serum-free medium (G_1) or were stimulated with serum (SS; S-phase) after which the SAC was loaded with C_6NBD-GalCer as described in detail in Materials and Methods. Following the subsequent 20-min chase of the fluorescent probe from the SAC, the percentage cells that displayed a fluorescently (i.e. NBD) labeled bile canalicular pole (BCP) (i.e. cells with fluorescent label in either only SAC, only BC, or SAC + BC) was determined as described in Materials and Methods. The relative distribution of the probe within the labeled BCP was then categorized as derived from SAC alone, BC alone of from both SAC and BC. Data are expressed as mean +/- SD of at least three independent experiments carroed out in duplicate. * $p<0.05$.

G_1-S-phase transition inhibits OSM-stimulated recruitment of PKA to the centrosomal region

The ability of OSM to activate SAC-to-apical surface route requires cAMP/PKA activity, as evidenced by using pharmacological inhibitors of PKA (van der Wouden et al., 2002). Although OSM did not give rise to increased cAMP or PKA expression levels, a significant recruitment of PKA to the centrosome region was noted (van der Wouden et al., 2002). In order to determine whether the OSM-stimulated recruitment of PKA to the centrosome region corresponds to its ability to activate the SAC-to-BC pathway, we examined the effect of G_1-S-phase transition on the ability of OSM to stimulate centrosomal PKA recruitment. For this, cells were synchronized in G_1 by serum deprivation and, subsequently, incubated for 4 h in serum-free medium (which maintains the cells in G_1), or in FCS-containing medium (which drives the cells into the S-phase), both supplemented with OSM. Cells were then fixed and stained with antibodies raised against the centrosomal protein γ-tubulin and PKA. The percentage of PKA-positive centrosomes (identified by γ-tubulin) was then determined. As shown in table 2, OSM stimulated the recruitment of PKA to centrosome region in G_1 cells (~24% more γ-tubulin-labeled centrosomes were positive for PKA). Illustrative immunofluorescence pictures are shown in Figure 7A-F. In striking contrast, OSM failed to recruit PKA to the centrosome region in S-phase cells (table 2). In fact, 13% less γ-tubulin-labeled centrosomes in serum-stimulated cells displayed PKA association, and OSM failed to stimulate PKA recruiment at the centrosomal region (table 2; Figure 7G-L). In serum-stimulated cells, but not in serum-deprived cells, some PKA localized to the nucleus. Given that PKA is required for OSM to activate the SAC-to-BC transport pathway and apical PM biogenesis, the apparent inability of OSM to recruit PKA to the centrosome region upon G_1-S-phase transition is likely to be part

of the underlying mechanism responsible for rendering the cells insensitive to OSM with regard to apical PM biogenesis.

	% increase in PKA-positive centrosomes
Control	0
OSM	+ 24 +/- 4 *
SS-control	- 13 +/- 4 *
SS-OSM	- 12 +/- 3 *

* $p<0.01$ (OSM vs. control; SS-control vs. control; SS-OSM vs. OSM)

Table 2 Effect of serum-stimulated G_1-S-phase transition on OSM-stimulated recruitment of PKA to the centrosomal region. Serum-deprived cells were kept in serum-free medium (to keep them in G_1) or were stimulated with serum (to drive them in the S-phase) in the presence or absence of OSM. The cells were then fixed and labeled with antibodies against γ-tubulin and PKA as described in Materials and Methods. The percentage of γ-tubulin-positive centrosomes that were labeled with PKA was determined. Data are expressed as mean +/- SEM of two independent experiments carried out in duplicate. Representative images of the quantitative results are shown in Figure 7.

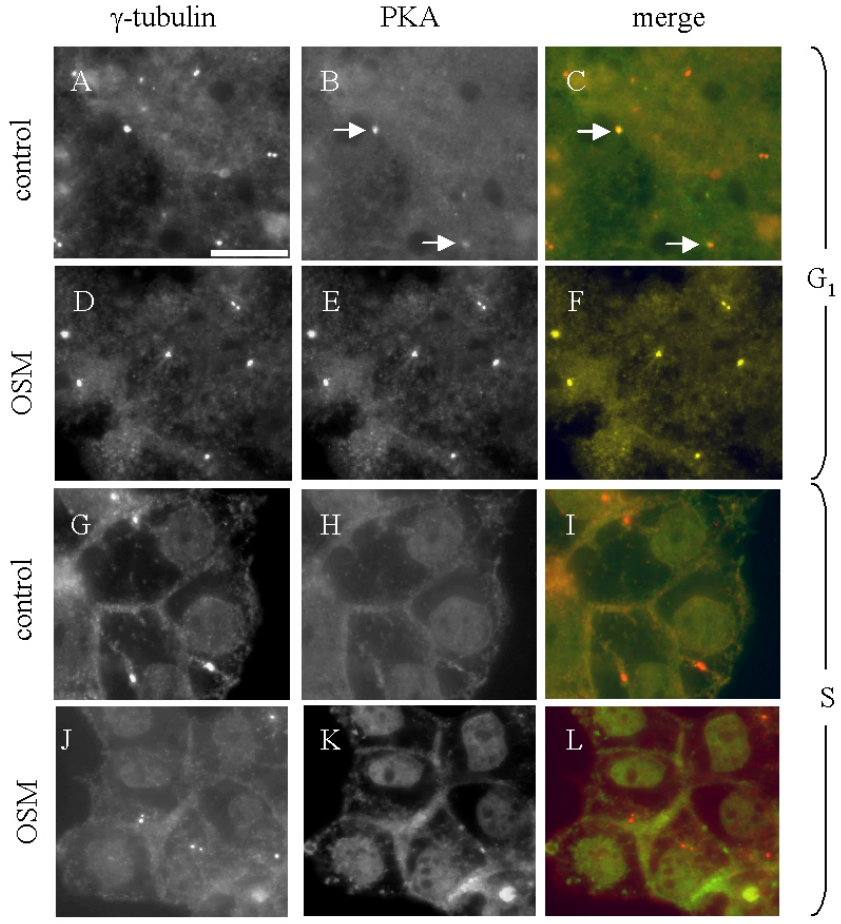

Figure 7 Effect of serum-stimulated G_1-S-phase transition on OSM-stimulated recruitment of PKA to the centrosomal region. Serum-deprived cells were kept in serum-free medium (to keep them in G_1; A-F) or were stimulated with serum (to drive them in the S-phase; G-L) in the presence (D-F, J-L) or absence (A-C, G-I) of OSM. The cells were then fixed and labeled with antibodies against γ-tubulin and PKA as described in Materials and Methods. The percentage of γ-tubulin-positive centrosomes that were labeled with PKA was determined and representative pictures were taken. Note that OSM stimulates the recruitment of PKA to γ-tubulin-positive centrosomes (dotted appearance) in G_1 cells (compare D-F to A-C) but not in S-phase cells (compare J-L to G-I). Arrows in B and C point to centrosomes positive for both γ-tubulin and PKA. In D-F, all γ-tubulin-positive centrosomes shown are also positive for PKA. C, F, I, L show merged images with γ-tubulin in red and PKA in green. Bars 10 µm.

Discussion

In this study, we have addressed the functional relationship between cell cycle regulation and the acquisition of a polarized phenotype, i.e. apical PM biogenesis, in hepatic HepG2 cells in response to OSM signaling. First, we demonstrate that (OSM-stimulated) apical PM biogenesis in HepG2 cells displays a strong positive correlation with expression levels of the cell cycle regulatory protein $p27^{Kip1}$ and subsequent G_1-phase arrest. Indeed, exposure of the cells to OSM enhances the expression of $p27^{Kip1}$ and prevents entry of the cells in S-phase as evidenced by the inhibition of BrdU incorporation (Figure 2). This is in agreement with the findings of Klausen et al (2000), which showed that OSM inhibits cell cycle progression by preventing $p27^{Kip1}$ degradation in HepG2 cells. Importantly, our data indicate that apical PM biogenesis stimulated by OSM is critically dependent on the ability of OSM to control $p27^{Kip1}$/ cdk2-mediated G_1-S-phase progression. Thus, asynchronous cells readily respond to OSM signaling with regard to apical PM biogenesis, and both serum deprivation, which results in increased $p27^{Kip1}$ expression, and synchronization of the cells in G_1-phase enhances the stimulatory effect of OSM (Figure 3). In striking contrast, serum- or FB1-stimulated downregulation of $p27^{Kip1}$ expression levels allowing G_1-S-phase transition to occur, effectively renders the cells insensitive to the cell polarity-stimulating effects of OSM (Figure 2, 3). $p27^{Kip1}$ downregulation results in an expected net increase in cdk2 activity, which plays an important role in G_1-S-phase transition (Ekholm and Reed, 2000; Woo and Poon, 2003). Inhibition of cdk2 activity in HepG2 cells with roscovitin prevented G_1-S-phase transition and kept the cells responsive to the polarity-stimulating effects of OSM, even in the serum- or FB1-treated cells. Together, our data indicate that extracellular signal- and $p27^{Kip1}$/ cdk2-regulated cell cycle progression controls *de novo* apicalization of the cell surface.

G_1-to-S phase transition is marked by two key events: initiation of DNA replication and centrosome duplication, both of which are controled by cdk2 activity (Matsumoto et al., 1999; Hinchcliffe and Sluder, 2002; Okuda, 2002). In order to determine whether the acquired insensitivity of the cells during G_1-S-phase transition could be specifically correlated to either of these two events we treated the cells with hydroxyurea. Hydroxyurea inactivates ribonucleoside reductase thereby blocking the synthesis of deoxynucleotides, which inhibits DNA synthesis (Yarbro, 1992) and induces synchronization of the cells in S-phase (Chouteau et al., 2001; Khodjakov et al., 2002). Importantly, by contrast, hydroxyurea does not block the process of centrosome duplication (Balczon et al., 1995; Khodjakov et al., 2002), allowing discrimination between the two events. Hydroxyurea-mediated inhibition of DNA synthesis rendered the cells insensitive to the polarity-stimulating effects of OSM to a similar extent as serum- or FB1-stimulated G_1-S-phase transition. This suggests that cdk2-stimulated centrosome cycle progression, i.e. centriole duplication/ replication, rather than DNA synthesis, coincides with the acquired insensitivity of the cells to OSM-stimulated apical PM biogenesis.

The results obtained from hydroxyurea-treated cells suggest that OSM, because of its ability to regulate $p27^{Kip1}$/ cdk2 activity, may act as a novel inhibitory modulator of centrosome cycle progression at the G_1/S boundary. This is supported by our previous observation that treatment with OSM induces the recruitment of protein kinase A (PKA) to the centrosomal region in HepG2 cells (van der Wouden et al., 2002). Serum-triggered G_1-S-phase transition effectively inhibits the OSM-stimulated recruitment of PKA to the centrosomal region (table 2; Figure 7). This is in agreement with the finding that the displacement of PKA from centrosomes positively modulates G_1-S-phase transition (Feliciello et al., 2000). Interestingly, very similar to the observed inhibition of *de novo* polarity development upon G_1-S-phase transition (Figures 3, 4), the stimulatory effect of OSM on

apical PM biogenesis in HepG2 cells is abolished when cAMP/PKA activity is inhibited (van der Wouden et al., 2002). At present, a molecular link between cdk2 activity at the G_1/S-boundary and PKA association at the centrosome is unclear. However, such a link is not unprecedented as mitotic CDK1 activity has been demonstrated to displace PKA from centrosomal A-kinase anchoring proteins (AKAPs). Current research in our lab is focussed at the molecular mechanism by which OSM stimulates PKA recruitment to the centrosomal region and the identification of OSM-controled PKA targets.

Centrosomes have been implicated in all microtubule-dependent processes including mitotic spindle positioning, cell shape, cell motility and polarity and organelle transport (Meraldi and Nigg, 2002). The Golgi apparatus and SAC are typically concentrated in the centrosome region, and both the centrosome and associated organelles typically face specialized cell surface domains, e.g. the leading lamella in migrating fibroblasts (Ueda et al., 1997) and the apical PM domain in epithelial cells (Buendia et al., 1990). Moreover, in differentiated G_1 cells, one of the centrosomes moves to the apical surface to form the basal body of the primary cilium, a highly specialized membrane domain that extends from the apical surface. The functional relevance for the clustering of Golgi and SAC around the centrosome is not clear. Recent evidence, however, suggest that the centrosome positions organelles in close proximity to specific target membranes. This may then facilitate or reinforce cytoskeleton remodeling and/ or membrane exchange between organelles and the cell surface necessary for the biogenesis of specialized PM domains, such as the apical surface (Wald et al. 2003) or the furrow during cytokinesis (Riggs et al., 2003). OSM-stimulated membrane trafficking from SAC to the developing apical surface requires microtubules (our unpublished results). Serum-stimulated G_1-S-phase transition did not visibly affect the spatial organization of SAC (Figure 6) and also the distribution of the microtubule cytoskeleton was not visibly altered (data not shown), indicating

that serum-stimulated cells had not reached prophase during which duplicated centrosomes separate and microtubules are rearranged to form spindles. Despite the lack of microtubule reorganization, serum-stimulated G_1-S-phase transition effectively inhibited the OSM-stimulated and PKA-dependent activation of a membrane transport pathway exiting the SAC and directed towards the developing apical surface (table 1; Figure 6), and inhibited OSM-stimulated recruitment of PKA to the centrosomal region (table 2; Figure 7). Our data suggest that recruitment of PKA to the centrosomal region is required for OSM to activate a membrane traffic route from SAC to the developing apical surface and, in this way, stimulating apical PM biogenesis. This underscores the importance of the centrosomal region as a specialized site where complex cellular events including cell cycle progression and membrane traffic are coordinately integrated (Rieder et al., 2001), and implicates OSM as an important regulating factor in this.

Based on these data, we propose a model (Figure 8) in which OSM signaling enhances $p27^{Kip1}$ expression and, consequently, downregulates cdk2 activity resulting in G_1 arrest. Low cdk2 activity allows OSM-stimulated recruitment of PKA to the centrosomal region which is essential for mediating the OSM-activated membrane exchanges between SAC and the developing apical surface. Upon G_1-S-phase transition, induced by circulating growth factors or mitogenic mycotoxins such as FB1 (this study; Schroeder et al., 1994), the increasing cdk2 activity may not be sufficiently downregulated by OSM and, therefore, interferes with OSM-mediated recruitment of PKA to the centrosomal region. This then impairs the regulated membrane supply from the pericentrosomal SAC to the cell surface and, hence, apical PM biogenesis. This model underscores the recently suggested role of endosomal recycling in the spatial-temporal control of plasma membrane insertion that is required for cell morphogenesis (Lequit, 2003; Pelissier et al., 2003), e.g. the development of the apical domain, and places PKA-regulated polarized plasma

membrane recycling under control of $p27^{Kip1}$/cdk2-regulated G_1-S-phase transition.

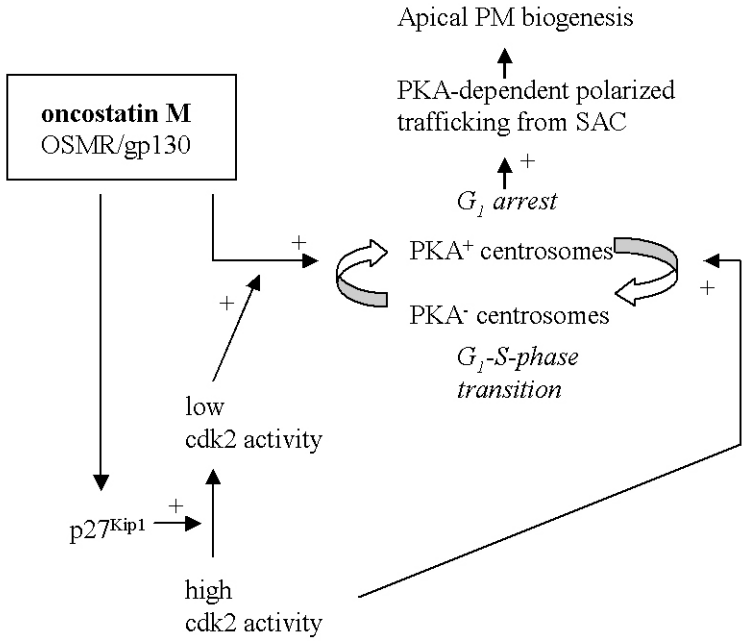

Figure 8 Working model. A detailed explanation is provided in the Discussion section.

Acknowledgments

S.C.D. van IJzendoorn was supported by the Royal Dutch Academy of Sciences (KNAW). We thank Karin Klappe for her help with the synthesis of C_6-NBD-labeled sphingolipids.